Hindawi Publishing Corporation
Abstract and Applied Analysis
Volume 2014, Article ID 317543, 5 pages
http://dx.doi.org/10.1155/2014/317543

Research Article

Travelling Wave Solutions of Nonlinear Dynamical Equations in a Double-Chain Model of DNA

Zheng-yong Ouyang[1] and Shan Zheng[2]

[1] *Department of Mathematics, Foshan University, Foshan Guangdong 528000, China*
[2] *Guangzhou Maritime College, Guangzhou Guangdong 510725, China*

Correspondence should be addressed to Zheng-yong Ouyang; zyouyang_math@163.com

Received 6 January 2014; Revised 24 February 2014; Accepted 10 March 2014; Published 3 April 2014

Academic Editor: Yonghui Xia

We consider the nonlinear dynamics in a double-chain model of DNA which consists of two long elastic homogeneous strands connected with each other by an elastic membrane. By using the method of dynamical systems, the bounded traveling wave solutions such as bell-shaped solitary waves and periodic waves for the coupled nonlinear dynamical equations of DNA model are obtained and simulated numerically. For the same wave speed, bell-shaped solitary waves of different heights are found to coexist.

1. Introduction

In 1953, Waston and Crick discovered the structure of deoxyribonucleic acid (DNA) double helix [1], which opened the area of molecular biology. The significance of the double helix model not only means the proven structure of DNA, but, more importantly, also helps to reveal the replication mechanism of DNA. To further study the characteristics of DNA, nonlinear science has been used to deal with DNA system, because its properties can be investigated by nonlinear models that combine the methods of physics with biological tools [2]. The soliton theory especially which pertains to nonlinear science has been widely applied in the study of DNA [3–6].

To study DNA structure from the view of nonlinear science, it is necessary to look for the right nonlinear mathematical models. A number of researchers have tried to establish mathematical models to describe DNA system. At the beginning, it is difficult to use a specific mathematical model to simulate DNA system due to its complex structure and the presence of various movements [7]. So some simplified models were used to study only some internal movement in DNA [8–12]. Further, two movements which made the main contribution to the DNA denaturation process were taken into account together in one model. For example, a two-dimensional discrete model was used to describe the two movements in DNA [13]. Another new double-chain model of DNA that consists of two long elastic homogeneous strands was given to describe transverse movements along the hydrogen bond and longitudinal movements along the backbone direction [14, 15].

In [14, 15], the nonlinear dynamical equations were derived and nonlinear dynamics of DNA were studied. The exact solutions of the general nonlinear dynamic system in the double-chain model of DNA were obtained and discussed numerically and analytically under some special approximate conditions. The nonlinear dynamical equations for the double-chain model were given as follows:

$$\begin{aligned} u_{tt} - c_1^2 u_{xx} &= \lambda_1 u + \gamma_1 uv + \mu_1 u^3 + \beta_1 uv^3, \\ v_{tt} - c_2^2 v_{xx} &= \lambda_2 v + \gamma_2 u^2 + \mu_2 u^2 v + \beta_2 v^3 + c_0, \end{aligned} \tag{1}$$

where u denotes the difference of the longitudinal displacements of the bottom and top strands, that is, the displacements of the bases from their equilibrium positions along the direction of the phosphodiester bridge that connects the two bases of the same strands; v represents the difference of the transverse displacements of the bottom and top strands, that is, the displacements of the bases from their equilibrium positions along the direction of the hydrogen bond that

connects the two bases of the base pair. The constants c_1, c_2, λ_1, λ_2, γ_1, γ_2, μ_1, μ_2, β_1, β_2, and c_0 in (1) are written as

$$c_1 = \pm\sqrt{\frac{Y}{\rho}}, \qquad c_2 = \pm\sqrt{\frac{F}{\rho}}, \qquad \lambda_1 = \frac{-2\mu}{\rho\sigma h}\left(h - l_0\right),$$
$$\lambda_2 = \frac{-2\mu}{\rho\sigma}, \qquad \gamma_1 = 2\gamma_2 = \frac{2\sqrt{2}\mu l_0}{\rho\sigma h^2}, \qquad \mu_1 = \mu_2 = \frac{-2\mu l_0}{\rho\sigma h^3},$$
$$\beta_1 = \beta_2 = \frac{4\mu l_0}{\rho\sigma h^3}, \qquad c_0 = \frac{\sqrt{2}\mu\left(h - l_0\right)}{\rho\sigma h}, \tag{2}$$

where $\rho, \sigma, Y, F, \mu, l_0$, and h are, respectively, the mass density, the area of transverse cross-section, the Young modulus, the tension density of the strand, the rigidity of the elastic membrane, the distance of the two strands, and the height of the membrane in the equilibrium position.

In [16], introducing the transformation $v = au + b$ (a and b are constants) in (1) yields

$$\begin{aligned} u_{tt} - c_1^2 u_{xx} &= u^3\left(\mu_1 + \beta_1 a^2\right) + u^2\left(2\beta_1 ab + a\gamma_1\right) \\ &\quad + u\left(\lambda_1 + b\gamma_1 + \beta_1 b^2\right), \\ u_{tt} - c_2^2 u_{xx} &= u^3\left(\mu_2 + \beta_2 a^2\right) + u^2\left(\frac{\gamma_2}{a} + \frac{\mu_2 b}{a} + 3\beta_2 ab\right) \\ &\quad + u\left(\lambda_2 + 3\beta_2 b^2\right) + \frac{\lambda_2 b}{a} + \frac{\beta_2 b^3}{a} + \frac{c_0}{a}. \end{aligned} \tag{3}$$

Comparing (3) and using the physical quantities (2), it follows that $b = h/\sqrt{2}$ and $F = Y$; (3) can be written as

$$u_{tt} - c_1^2 u_{xx} = Au^3 + Bu^2 + Cu + D, \tag{4}$$

where $A = ((-2\alpha/h^3) + (4a^2\alpha/h^3))$, $B = 6\sqrt{2}a\alpha/h^2$, $C = ((-2\alpha/l_0) + (6\alpha/h))$, and $D = 0$ with $\alpha = \mu l_0/\rho\sigma$.

Reference [16] studied the traveling wave solutions of (4) and obtained one particular family of solitary kink-type solutions for different values of Riccati parameter of (4). Unfortunately the results are not complete, because (4) admits tanh-type, periodic-type, and bell-type solutions; [16] only presented the tanh-type solutions.

In this paper, we use the bifurcation method of dynamical systems [17–20] to study bell-type and periodic-type solutions of (6), which can improve the results in [16]. We look for solutions of (4) in the form of $u(x,t) = \varphi(\xi)$ with $\xi = (x/c_1) - \sqrt{2}t$. Substituting $u(x,t) = \varphi((x/c_1) - \sqrt{2}t)$ into (4), we have

$$\varphi_{\xi\xi} = A\varphi^3 + B\varphi^2 + C\varphi, \tag{5}$$

which is equivalent to the following two-dimensional system:

$$\frac{d\varphi}{d\xi} = y, \qquad \frac{dy}{d\xi} = A\varphi^3 + B\varphi^2 + C\varphi. \tag{6}$$

Obviously, system (6) has the first integral

$$H(\varphi, y) = \frac{1}{4}A\varphi^4 + \frac{1}{3}B\varphi^3 + \frac{1}{2}C\varphi^2 - \frac{1}{2}y^2 = M, \tag{7}$$

where M is the Hamiltonian constant.

In fact, system (6) is a planar dynamical system whose phase orbits defined by the vector field of (6) determine traveling wave solutions, so we first need to investigate some different phase portraits of system (6) in different parameter regions. Then, by using the theory of dynamical system, we will identify some different wave profiles and compute exact representations for solitary wave solutions and periodic wave solutions.

This paper is organized as follows. In Section 2, we draw bifurcation phase portraits of system (6), where explicit parametric conditions will be derived. In Section 3, we give exact representations of solitary wave and periodic wave solutions of (6) in explicit form. A short conclusion will be given in Section 4.

2. Properties of Singular Points and Bifurcation Phase Portraits

Firstly, we compute the equilibrium points of system (6) under different parametric conditions. It is clear that neither the parameters B nor C takes value zero from the forms of parameters A, B, and C; then A equals zero if $a = \pm\sqrt{2}/2$. So we give equilibrium points in different parametric cases as follows.

(1) When $A = 0$, there are two equilibrium points $(0,0)$ and $(-C/B, 0)$.

(2) When $A \neq 0$ and $\delta_1 > 0$, there are three equilibrium points $(0,0)$, $(\varphi_-, 0)$, and $(\varphi_+, 0)$ of (6) on the φ-axis, where $\delta_1 = B^2 - 4AC$, $\varphi_- = (-B - \sqrt{\delta_1})/2A$, and $\varphi_+ = (-B + \sqrt{\delta_1})/2A$.

Define $f_0(\varphi) = A\varphi^3 + B\varphi^2 + C\varphi$; then the type of equilibrium point $(\varphi, 0)$ can be decided by $\lambda_\pm = \sqrt{f_0'(\varphi)}$, which are eigenvalues of linearized system of (6) at point $(\varphi, 0)$.

Secondly, we compute the intersection points of phase portraits of (6) on the φ-axis when the orbits pass through the equilibrium point $(0,0)$, namely, when the Hamiltonian constant $M = h(0,0) = 0$. Let $f(\varphi) = (1/2)A\varphi^4 + (2/3)B\varphi^3 + C\varphi^2$, $\delta_2 = (4/9)B^2 - 2AC$, $\varphi_0 = -3A/2B$, $\varphi_1 = ((-2/3)B - \sqrt{\delta_2})/A$, and $\varphi_2 = ((-2/3)B + \sqrt{\delta_2})/A$. When $A = 0$, there are a double zero point 0 and a zero point φ_0 of $f(\varphi)$ on the φ-axis. When $A \neq 0$ and $\delta_2 > 0$, there are a double zero point 0 and two zero points φ_1 and φ_2 of $f(\varphi)$ on the φ-axis. In order to draw bifurcation phase portraits of system (6), we need to discuss the sign of parameters A, B, and C. The intersection points of phase portraits of (6) on the φ-axis are given as follows.

(1) If $A = 0$, there are two intersection points $(0,0)$ and $(\varphi_0, 0)$ of (6) on the φ-axis (see Figure 1).

(2) If $A > 0$, there are three intersection points $(0,0)$, $(\varphi_1, 0)$, and $(\varphi_2, 0)$ of (6) on the φ-axis and $\varphi_1 < \varphi_2$ (see Figure 2).

(3) If $A < 0$, there are three intersection points $(0,0)$, $(\varphi_1, 0)$, and $(\varphi_2, 0)$ of (6) on the φ-axis and $\varphi_2 < \varphi_1$ (see Figure 3).

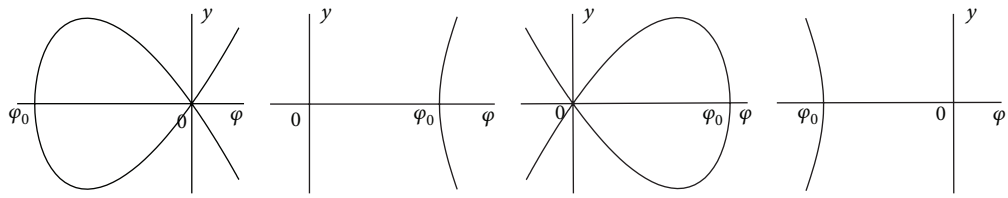

(a) $B > 0, C > 0$ (b) $B > 0, C < 0$ (c) $B < 0, C > 0$ (d) $B < 0, C < 0$

Figure 1: The bifurcation phase portraits of system (6) with $A = 0$.

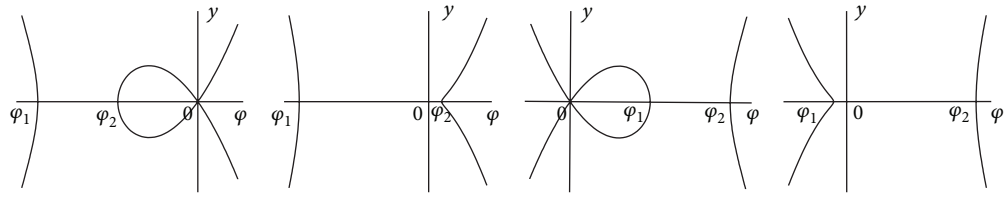

(a) $B > 0, C > 0$ (b) $B > 0, C < 0$ (c) $B < 0, C > 0$ (d) $B < 0, C < 0$

Figure 2: The bifurcation phase portraits of system (6) with $A > 0$.

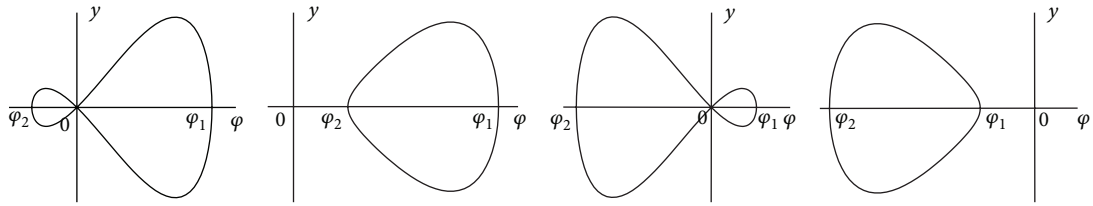

(a) $B > 0, C > 0$ (b) $B > 0, C < 0$ (c) $B < 0, C > 0$ (d) $B < 0, C < 0$

Figure 3: The bifurcation phase portraits of system (6) with $A < 0$.

Finally, from the above analysis about system (6), we give twelve different phase portraits of (6) which are shown in Figures 1–3. There exist homoclinic orbits and periodic orbits in some phase portraits of Figures 1–3, which correspond to bell-type and periodic-type waves and are of special interest to us.

3. Exact Explicit Representations of Solitary Wave Solutions

(1) The case $A = 0$, $B > 0$, and $C > 0$ (see Figure 1(a)).

Corresponding to the homoclinic orbit of (6) passing through points $(\varphi_0, 0)$ and $(0, 0)$ on the $\varphi - y$ plane, there exists a smooth solitary wave solution. Now, (7) becomes

$$y^2 = \frac{2}{3}B\varphi^3 + C\varphi^2 \quad (\varphi_0 \leqslant \varphi \leqslant 0). \tag{8}$$

Choosing $\varphi(0) = \varphi_0$, substituting (8) into the first equation of (6), and integrating along the homoclinic orbit, we have

$$\int_{\varphi}^{\varphi_0} \frac{1}{s\sqrt{(2/3)\,Bs + C}}\,ds = |\xi|. \tag{9}$$

Solving (9) yields

$$u_1 = -\frac{3C}{B\left(\cosh\left(\sqrt{C}\,|\xi|\right) + 1\right)}. \tag{10}$$

(2) The case $A = 0$, $B < 0$, and $C > 0$ (see Figure 1(c)).

Similarly, in Figure 1(c) the homoclinic orbit has the following expression:

$$y^2 = \frac{2}{3}B\varphi^3 + C\varphi^2 \quad (0 \leqslant \varphi \leqslant \varphi_0). \tag{11}$$

Thus the corresponding smooth solitary wave solution is obtained as (10) and its profile is shown in Figure 4(b).

(3) The case $A > 0$, $B > 0$, and $C > 0$ (see Figure 2(a)).

In this case, on the $\varphi - y$ plane the homoclinic orbit of (6) passing through points $(\varphi_2, 0)$ and $(0, 0)$ has the following expression:

$$y^2 = \frac{1}{2}A\varphi^4 + \frac{2}{3}B\varphi^3 + C\varphi^2 \quad (\varphi_2 \leqslant \varphi \leqslant 0). \tag{12}$$

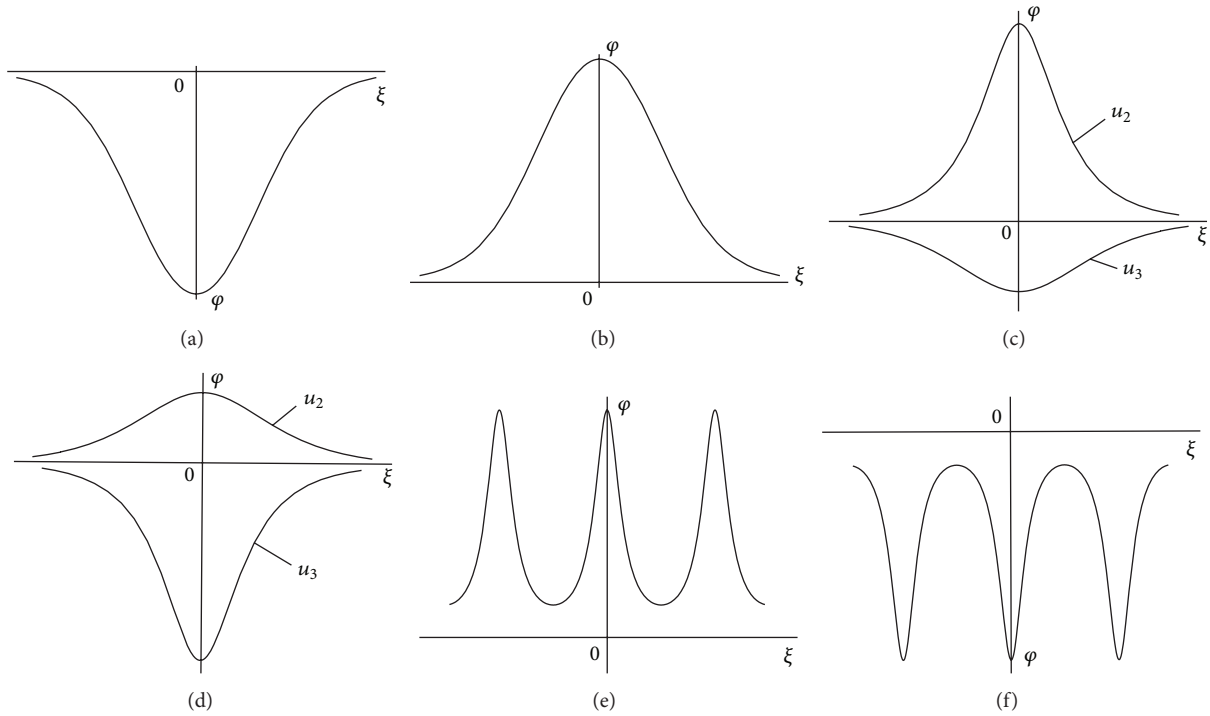

Figure 4: Smooth solitary wave and periodic wave solutions.

Choosing $\varphi(0) = \varphi_2$, substituting (12) into the first equation of (6), and integrating along the homoclinic orbit, we have

$$\int_{\varphi}^{\varphi_2} \frac{1}{s\sqrt{(1/2)\,As^2 + (2/3)\,Bs + C}}\,ds = |\xi|. \tag{13}$$

Solving (13), it follows that

$$u_2 = \frac{4C\alpha_1}{\alpha_1^2 e^{-\sqrt{C}|\xi|} + \left((4/9)\,B^2 - 2AC\right)e^{\sqrt{C}|\xi|} - (4/3)\,B\alpha_1}, \tag{14}$$

where $\alpha_1 = (2(-2B^2 + 9AC + B\sqrt{4B^2 - 18AC}))/(-6B + 3\sqrt{4B^2 - 18AC})$. The profiles of solutions u_1 and u_2 both have figure caption Figure 4(a).

(4) The case $A > 0$, $B < 0$, and $C > 0$ (see Figure 2(c)).

In this case, on the $\varphi - y$ plane the homoclinic orbit of (6) passing through points $(\varphi_1, 0)$ and $(0, 0)$ has the following expression:

$$y^2 = \frac{1}{2}A\varphi^4 + \frac{2}{3}B\varphi^3 + C\varphi^2 \quad \left(0 \leqslant \varphi \leqslant \varphi_1\right). \tag{15}$$

Choosing $\varphi(0) = \varphi_1$, substituting (15) into the first equation of (6), and integrating along the homoclinic orbit, we have

$$\int_{\varphi}^{\varphi_1} \frac{1}{s\sqrt{(1/2)\,As^2 + (2/3)\,Bs + C}}\,ds = |\xi|. \tag{16}$$

Solving (16), we get

$$u_3 = \frac{4C\alpha_2}{\alpha_2^2 e^{\sqrt{C}|\xi|} + \left((4/9)\,B^2 - 2AC\right)e^{-\sqrt{C}|\xi|} - (4/3)\,B\alpha_2}, \tag{17}$$

where $\alpha_2 = (2(2B^2 - 9AC + B\sqrt{4B^2 - 18AC}))/(6B + 3\sqrt{4B^2 - 18AC})$. The profile of u_3 is shown in Figure 4(d).

(5) The case $A < 0$, $B > 0$, and $C > 0$ and $A < 0$, $B < 0$, and $C > 0$ (see Figures 3(a) and 3(c)).

In this case, there exist two homoclinic orbits and their expressions are (12) and (15), respectively. Similarly we get the corresponding solitary wave solutions as u_2 and u_3, which coexist for the same speed. The plane graphs of the coexisting solitary wave solutions are shown in Figure 4(c), when $A < 0$, $B > 0$, and $C > 0$, and Figure 4(d), when $A < 0$, $B < 0$, and $C > 0$.

(6) The case $A < 0$, $B > 0$, and $C < 0$ (see Figure 3(b)).

In this case, on the $\varphi - y$ plane the orbit of (6) which passes through points $(\varphi_1, 0)$ and $(\varphi_2, 0)$ is a periodic orbit; it has the following expression:

$$y^2 = \frac{1}{2}A\varphi^4 + \frac{2}{3}B\varphi^3 + C\varphi^2, \quad \left(0 < \varphi_2 \leqslant \varphi \leqslant \varphi_1\right). \tag{18}$$

Choosing $\varphi(0) = \varphi_1$, substituting (18) into the first equation of (6), and integrating along the periodic orbit, we have

$$\int_{\varphi}^{\varphi_1} \frac{1}{s\sqrt{(1/2)\,As^2 + (2/3)\,Bs + C}}\,ds = |\xi|. \tag{19}$$

Solving (19) we obtain the following periodic wave solution:

$$u_4 = \frac{6C}{\sqrt{4B^2 - 18AC}\cos\left(\sqrt{-C}\xi\right) - 2B}. \tag{20}$$

The profile of u_4 is shown in Figure 4(e).

(7) The case $A < 0$, $B < 0$, and $C < 0$ (see Figure 3(d)).

Similarly, corresponding to the periodic orbit of (6) which passes through points $(\varphi_1, 0)$ and $(\varphi_2, 0)$, there exists a periodic wave solution. Now, the expression of the periodic orbit is

$$y^2 = \frac{1}{2}A\varphi^4 + \frac{2}{3}B\varphi^3 + C\varphi^2, \quad (\varphi_2 \leqslant \varphi \leqslant \varphi_1 < 0). \tag{21}$$

Choosing $\varphi(0) = \varphi_2$, substituting (21) into the first equation of (6), and integrating along the periodic orbit, we have

$$\int_{\varphi_2}^{\varphi} \frac{1}{s\sqrt{(1/2)\,As^2 + (2/3)\,Bs + C}}\,ds = |\xi|. \tag{22}$$

Solving (22), it follows that

$$u_5 = \frac{6C}{-\sqrt{4B^2 - 18AC}\cos\left(\sqrt{-C}\xi\right) - 2B}. \tag{23}$$

The profile of u_5 is shown in Figure 4(f).

4. Conclusion

In this paper, we employ the method of dynamical systems to study the nonlinear dynamical equations of DNA model. The bifurcation phase portraits of the DNA under some parametric conditions are drawn, and explicit exact expressions of bell-shaped solitary waves and periodic waves are obtained via some special homoclinic and periodic orbits; their planar graphs are simulated. These solutions are new and different from those in [14–16]; some existing results are improved. Furthermore, in general, the larger the wave speed, the higher the wave crest. So for the same wave speed, it is interesting that the bell-shaped solitary waves of different heights are found to coexist.

Conflict of Interests

The authors declare that there is no conflict of interests regarding the publication of this paper.

Acknowledgments

This work was supported by the National Natural Science Foundation of China (no. 11226303) and Guangdong Province (no. 2013KJCX0189). The authors thank the editors for their hard working and also gratefully acknowledge helpful comments and suggestions by reviewers.

References

[1] J. D. Watson and F. H. C. Crick, "Molecular structure of nucleic acids: a structure for deoxyribose nucleic acid," *Nature*, vol. 171, no. 4356, pp. 737–738, 1953.

[2] M. Peyrard, S. C. López, and G. James, "Modelling DNA at the mesoscale: a challenge for nonlinear science?" *Nonlinearity*, vol. 21, p. T91, 2008.

[3] T. Lipniacki, "Chemically driven traveling waves in DNA," *Physical Review E*, vol. 60, p. 7253, 1999.

[4] S. Yomosa, "Solitary excitations in deoxyribonuclei acid (DNA) double helices," *Physical Review A*, vol. 30, no. 1, pp. 474–480, 1984.

[5] C. T. Zhang, "Soliton excitations in deoxyribonucleic acid (DNA) double helices," *Physical Review A*, vol. 35, no. 2, pp. 886–891, 1987.

[6] K. Forinash, "Nonlinear dynamics in a double-chain model of DNA," *Physical Review B*, vol. 43, p. 10734, 1991.

[7] L. V. Yakushevich, *Nonlinear Physics of DNA*, John Wiley & Sons, Berlin, Germany, 2004.

[8] S. W. Englander, N. R. Kallenbanch, A. J. Heeger, J. A. Krumhansl, and S. Litwin, "Nature of the open state in long polynucleotide double helices: possibility of soliton excitations," *Proceedings of the National Academy of Sciences of the United States of America*, vol. 77, pp. 7222–7226, 1980.

[9] S. Yomosa, "Soliton excitations in deoxyribonucleic acid (DNA) double helices," *Physical Review A*, vol. 27, no. 4, pp. 2120–2125, 1983.

[10] S. Takeno and S. Homma, "A coupled base-rotator model for structure and dynamics of DNA—local fluctuations in helical twist angles and topological solitons," *Progress of Theoretical Physics*, vol. 72, no. 4, pp. 679–693, 1984.

[11] M. Peyrard and A. R. Bishop, "Statistical mechanics of a nonlinear model for DNA denaturation," *Physical Review Letters*, vol. 62, no. 23, pp. 2755–2758, 1989.

[12] T. Dauxois, M. Peyrard, and A. R. Bishop, "Entropy-driven DNA denaturation," *Physical Review E*, vol. 47, no. 1, pp. R44–R47, 1993.

[13] V. Muto, P. S. Lomdahl, and P. L. Christiansen, "Two-dimensional discrete model for DNA dynamics: longitudinal wave propagation and denaturation," *Physical Review A*, vol. 42, no. 12, pp. 7452–7458, 1990.

[14] D. X. Kong, S. Y. Lou, and J. Zeng, "Nonlinear dynamics in a new double Chain-model of DNA," *Communications in Theoretical Physics*, vol. 36, no. 6, pp. 737–742, 2001.

[15] X.-M. Qian and S.-Y. Lou, "Exact solutions of nonlinear dynamics equation in a new double-chain model of DNA," *Communications in Theoretical Physics*, vol. 39, no. 4, pp. 501–505, 2003.

[16] W. Alka, A. Goyal, and C. Nagaraja Kumar, "Nonlinear dynamics of DNA—riccati generalized solitary wave solutions," *Physics Letters A: General, Atomic and Solid State Physics*, vol. 375, no. 3, pp. 480–483, 2011.

[17] S. N. Chow and J. K. Hale, *Methods of Bifurcation Theory*, Springer, Berlin, Germany, 1981.

[18] J. B. Li and Z. R. Liu, "Smooth and non-smooth traveling waves in a nonlinearly dispersive equation," *Applied Mathematical Modelling*, vol. 25, pp. 41–56, 2000.

[19] J. B. Li and Z. R. Liu, "Traveling wave solutions for a class of nonlinear dispersive equations," *Chinese Annals of Mathematics*, vol. 23, p. 397, 2002.

[20] Z. R. Liu and Z. Y. Ouyang, "A note on solitary waves for modified forms of Camassa-Holm and Degasperis-Procesi equations," *Physics Letters A*, vol. 366, no. 4-5, pp. 377–381, 2007.